ELSEVIER

The Spine Journal 10 (2010) 497–504

THE SPINE JOURNAL

Basic Science

Three-dimensional dynamic in vivo motion of the cervical spine: assessment of measurement accuracy and preliminary findings

Colin P. McDonald, PhD[a,*], Casey C. Bachison, MD[b], Victor Chang, MD[c], Stephen W. Bartol, MD[b], Michael J. Bey, PhD[a]

[a]*Bone and Joint Center, Henry Ford Hospital, Detroit, MI 48202, USA*
[b]*Department of Orthopaedic Surgery, Henry Ford Hospital, Detroit, MI 48202, USA*
[c]*Department of Neurosurgery, Henry Ford Hospital, Detroit, MI 48202, USA*

Received 5 October 2009; revised 18 January 2010; accepted 18 February 2010

Abstract

BACKGROUND CONTEXT: Previous research has quantified cervical spine motion with conventional measurement techniques (eg, cadaveric studies, motion capture systems, and fluoroscopy), but these techniques were not designed to accurately measure three-dimensional (3D) dynamic cervical spine motion under in vivo conditions.

PURPOSE: The purposes of this study were to characterize the accuracy of model-based tracking for measuring 3D dynamic cervical spine kinematics and to demonstrate its in vivo application.

STUDY DESIGN: Through accuracy assessment and application of technique, in vivo cervical spine motion was measured.

METHODS: The accuracy of model-based tracking for measuring cervical spine motion was determined in an in vitro experiment. Tantalum beads were implanted into the vertebrae of an ovine specimen, and biplane X-ray images were acquired as the specimen's neck was manually moved through neck extension and axial neck rotation. The 3D position and orientation of each cervical vertebra were determined from the biplane X-ray images using model-based tracking. For comparison, the position and orientation of each vertebra were also determined by tracking the position of the implanted beads with dynamic radiostereometric analysis. To demonstrate in vivo application of this technique, biplane X-ray images were acquired as a human subject performed two motion tasks: neck extension and axial neck rotation. The positions and orientations of each cervical vertebra were determined with model-based tracking. Cervical spine motion was reported with standard kinematic descriptions of translation and rotation.

RESULTS: The in vitro validation demonstrated that model-based tracking is accurate to within ± 0.6 mm and $\pm 0.6^{\circ}$ for measuring cervical spine motion. For the in vivo application, there were significant rotations about all three anatomical axes for both the neck extension and axial neck rotation motion tasks.

CONCLUSIONS: Model-based tracking is an accurate technique for measuring in vivo, 3D, dynamic cervical spine motion. Preliminary data acquired using this technique are in agreement with previous studies. It is anticipated that this experimental approach will enhance our understanding of cervical spine motion under normal and pathologic conditions.

Keywords: Cervical spine; Motion analysis; Validation; In vivo; Dynamic

Introduction

The cervical spine is a complex system of vertebral bones, intervertebral discs, muscles, and ligaments. Motion of the cervical spine is accomplished by the relative movement of seven motion segments (ie, two adjacent vertebral bodies and an intervertebral disc), and each motion segment contributes uniquely to the movement of the cervical spine.

FDA device/drug status: not applicable.

Author disclosures: SWB (private investments, including venture capital, start-ups, ISS Spine; other office, Musculoskeletal Transplant Foundation Medical Board of Trustees).

* Corresponding author. Bone and Joint Center, Henry Ford Hospital, 2799 W. Grand Blvd, E&R 2015, Detroit, MI 48202, USA. Tel.: (313) 916-2130; fax: (313) 916-8812.

E-mail address: cmcdona2@hfhs.org (C.P. McDonald)

1529-9430/$ – see front matter
doi:10.1016/j.spinee.2010.02.024

Significant research efforts have focused on measuring cervical spine motion in an effort to understand normal motion patterns and the manner in which these motion patterns are affected by pathologic conditions (eg, degenerative disc disease) and treatment. However, accurately measuring cervical spine motion during functional activities—particularly under in vivo conditions—remains a significant challenge.

Previous research has relied on a variety of experimental approaches for quantifying cervical spine motion. These include conventional motion capture systems [1,2], cadaveric studies [3,4], static imaging techniques [5–14], and two-dimensional (2D) dynamic imaging techniques [15,16]. Conventional motion capture systems that record the position of skin-mounted markers or sensors are capable of recording data under a wide variety of dynamic in vivo conditions. However, the externally positioned markers are susceptible to errors introduced by skin movement, and therefore, this approach is highly limited in the accuracy with which it can measure the motion of individual vertebrae. Cadaveric studies are capable of providing highly accurate measures of joint position and motion but cannot accurately reproduce the joint forces, muscle forces, and complex motion patterns associated with in vivo conditions. Two-dimensional radiography (ie, conventional X-ray imaging) has contributed extensively to the understanding of spine motion, but these studies have been restricted to intervertebral measurements at static neck positions. Furthermore, 2D imaging techniques are limited in their ability to accurately quantify out-of-plane motions. Static three-dimensional (3D) imaging has been performed with magnetic resonance imaging and computed tomography (CT), but these imaging modalities are largely restricted to acquiring static images as dynamic imaging systems are not yet widely available. Two-dimensional dynamic imaging studies (eg, fluoroscopy) can assess intervertebral translations and rotations throughout the full range of motion. However, these studies are again based on planar radiography and cannot characterize 3D motion with high levels of accuracy.

More recently, techniques have been reported that can measure in vivo, 3D spine motion. Dynamic radiostereometric analysis (RSA) has been used to measure 3D motion of the lumbar spine [17]. This technique provides highly accurate measures of 3D lumbar spine motion under in vivo conditions by tracking the 3D position of implanted tantalum beads from biplane X-ray images. However, the invasive nature of this technique (specifically, the implantation of tantalum beads under sterile conditions that is necessarily performed in conjunction with a surgical procedure) limits the number of willing study participants and ensures that the technique cannot be used to study normal motion or the effects of nonsurgical treatment. The validation of a dual fluoroscopy and an image-matching technique for measuring in vivo motion of the lumbar spine has also been reported [18]. This technique is promising because it does not rely on implanted tantalum beads and is capable of measuring 3D dynamic motion, but the accuracy with which this technique can measure rotations (a critical parameter in the assessment of vertebral motion) was not reported and is therefore unknown.

To overcome the limitations associated with previously reported techniques for measuring in vivo cervical spine motion, our laboratory has developed a method for tracking the motion of cervical vertebrae from biplane X-ray images based on their 3D shape and density. The objectives of this study were to characterize the translational and rotational accuracy of this measurement technique and to demonstrate its in vivo application. Based on previous experience with this technique, we expected that the model-based tracking technique would be accurate to within approximately 0.5 mm in translation and 1° in rotation.

Materials and methods

Overview

We have developed a technique for measuring 3D, dynamic, in vivo motion of the cervical spine. To validate this technique, we implanted tantalum beads into two vertebral bodies of an ovine cadaver specimen; recorded biplane radiographic images of the cervical spine while manually moving the specimen's neck; measured the 3D position and orientation of the two vertebrae using the model-based tracking technique; measured the 3D position and orientation of the two vertebrae by tracking the implanted tantalum beads with dynamic RSA; and then compared the results of the two techniques. The dynamic RSA method was used as the ''gold standard'' for comparison. Finally, one subject with no history of spine pathology or previous spine surgery was tested to demonstrate the in vivo application of this measurement technique.

Validation of model-based tracking technique

Four 1.6-mm-diameter tantalum beads were implanted into the third (C3) and fourth (C4) cervical vertebrae of one ovine cadaver specimen. The skull, the occiput, and cervical spine segments C1–C5 were available for testing. All soft tissues surrounding the vertebrae remained intact. The ovine cadaver specimen was selected for its ease of procurement, low cost, and similarity of the cervical vertebra in shape and size to those of the human cervical vertebra. The four tantalum beads were widely distributed throughout each vertebra. The instruments for implanting the markers consisted of matched stainless steel cannulas, inserts, and drill guides with depth stops. The cannula/insert was used to drill a hole through the bone at the proper angle and to the proper depth. The insert was removed, and a bead was inserted into the cannula surrounded by bone wax and pushed to the end of the hole. The position of each bead within bone was verified using static radiography. The specimen was secured to a custom apparatus with the

C3–C4 levels centered within the 3D imaging volume of a biplane X-ray system [19]. Biplane X-ray images were acquired as the specimen was manually moved through two motion tasks: neck extension and axial neck rotation. For the neck extension motion task, the head of the cadaver specimen was moved from a position of full flexion to full extension (Fig. 1, left). For the axial neck rotation motion task, the head was rotated from a position of maximal right rotation to maximal left rotation (Fig. 1, right). Three trials were conducted for each motion. Biplane X-ray images were also acquired for three static trials. The biplane X-ray images were acquired at 60 Hz for 2 seconds with the X-ray generators in pulsed mode (70 KV, 160 mA) and video cameras shuttered at 1/250 seconds to eliminate motion blur.

After testing, CT images were acquired using a clinical scanner (LightSpeed VCT; GE Medical Systems, New Berlin, WI, USA). Imaging parameters included a field of view of 130 mm, a 512×512 reconstruction matrix, and a voxel size of 0.25×0.25×1.25 mm. The CT images of the C3 and C4 vertebrae were then segmented from surrounding bones and soft tissues using commercial software (Mimics 12.0; Materialise, Leuven, Belgium) and reconstructed to generate a 3D bone model.

The 3D position and orientation of each cervical vertebra were determined from the biplane X-ray images using a model-based tracking technique [20]. Briefly, this technique generates a pair of digitally reconstructed radiographs by ray-traced projection through the CT bone model. The 3D position and orientation of a given bone can then be estimated by optimizing the correlation between the two digitally reconstructed radiographs and the two biplane X-ray images. This technique allowed for the independent determination of the 3D position and orientation of C3 relative to C4 for all frames of each trial. For comparison, the 3D position and orientation of C3 relative to C4 were also determined using the dynamic RSA technique [19]. This represented the gold standard position of C3 and C4 and was used to quantify the accuracy of the model-based tracking technique. This RSA technique has been shown to be accurate to within ±0.1 mm [19].

To report the accuracy of the model-based tracking technique in clinically relevant terms, an anatomical coordinate system was created with custom software for each vertebra (Fig. 2) [21]. To accomplish this, three anatomical landmarks were selected: the center of the vertebral body and the centers of the left and right lateral masses. The center of the vertebral body was determined by manually fitting a sphere to the vertebral body. The local anatomical coordinate system was defined by three orthogonal vectors. The left and right lateral mass points defined the lateral mass vector, which was nominally aligned in the medial-lateral (ML) direction. The X-axis (termed anterior-posterior [AP] axis) was defined as the midpoint of the lateral mass vector and the center of the vertebral body sphere and was oriented in the AP direction. The Z-axis (termed superior-inferior [SI] axis) was defined as the cross product of the AP-axis and the lateral mass vector and was oriented in the SI direction. Last, the Y-axis (termed ML-axis) was defined as the cross product of the SI-axis and the AP-axis and was oriented in the ML direction [21].

For each trial, 3D kinematics (ie, translations and rotations) of C3 relative to C4 were calculated based on the position and orientation data determined from the biplane X-ray images. Using the terminology reported by Stokes [21], lateral bending was defined as rotation about the AP-axis; flexion-extension was defined as rotation about the ML-axis; axial rotation was defined as rotation about the SI-axis; AP translation was defined as translation along

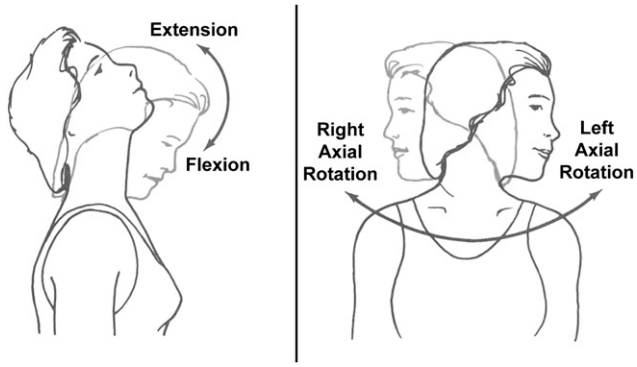

Fig. 1. Two motion activities were examined in this study. (Left) For the neck extension motion task, motion began with their neck in full flexion and extended to full extension. (Right) For the axial neck rotation motion task, motion began with the neck fully rotated to the right and then fully rotated to the left.

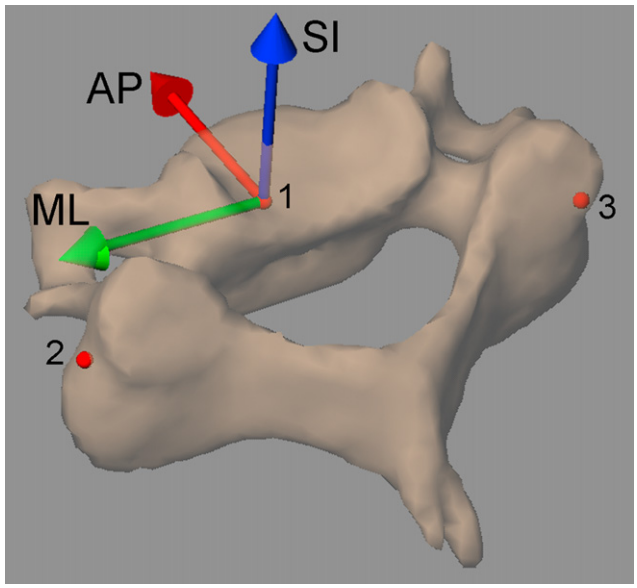

Fig. 2. An anatomical coordinate system was defined by three anatomical landmarks: (1) the center of the vertebral body and the centers of the (2) left and (3) right lateral masses. The anatomical coordinate system for each vertebra is aligned in the anterior-posterior (AP), medial-lateral (ML), and superior-inferior (SI) directions. A human C5 vertebra is shown.

the AP-axis; LR (left-right) translation was defined as translation along the ML-axis; and SI translation was defined as translation along the SI-axis. Expressing these kinematic data in a common anatomical coordinate system allows for a direct comparison between the model-based tracking and dynamic RSA techniques.

Translational and rotational accuracy were quantified in terms of bias and precision [22]. Bias was defined as the mean difference between the two measurement techniques (model-based tracking and dynamic RSA). Precision was defined as the standard deviation of the model-based measurements across all frames in the static trials. Additionally, overall dynamic accuracy was defined as the root mean square error between the two measurement techniques. Bias, precision, and dynamic accuracy were calculated for each of the six kinematic outcome measures. A *t* test was used to determine if the bias was significantly different than zero, with significance set at $p<.05$.

In vivo application

To demonstrate in vivo application of the model-based tracking technique, one subject (male, age 27 years) with no history of spine pathology or previous spine surgery was tested. Following Institute Review Board approval, the subject was seated with their neck centered in the biplane X-ray system. Biplane X-ray images were acquired at 60 Hz during two motion tasks: neck extension and axial neck rotation. For the neck extension motion task, the subject began with their neck in full flexion and extended to full extension (Fig. 1, left). For the axial neck rotation motion task, the subject began with their neck fully rotated to the right and then fully rotated to the left (Fig. 1, right). A static image was then recorded with the subject seated upright and facing forward to determine the neutral position. Three trials were collected per motion task.

To characterize the relationship between intervertebral motion (acquired with the biplane X-ray system) and gross head/neck motion, motion of the head relative to the torso was determined using a conventional video-based motion capture system. To accomplish this, spherical skin-mounted reflective markers were affixed to the subject's head and torso. On the head, three reflective markers were secured to the top of the skull (left, centered, and right) using a custom head mount. On the torso, reflective markers were secured to the left and right shoulders at the site of the acromion and at the base of the cervical spine on the upper back. During each motion task, the position of each reflective marker was simultaneously recorded at 60 Hz using a five-camera motion capture system (Motion Analysis Corp., Santa Rosa, CA, USA). The acquisition of the reflective surface marker data was synchronized with that of the biplane X-ray images. Using the same coordinate system notation defined for the individual vertebrae (Fig. 2), anatomical coordinate systems were created for both the head and torso that were aligned in the AP, ML, and SI directions. Using these coordinate systems, 3D rotations of the head with respect to the torso were calculated. Specifically, extension of the neck was defined as rotation about the torso's ML-axis, whereas axial rotation of the neck was defined as rotation about the torso's SI-axis. These neck rotations were calculated for each frame of every trial and were synchronized with the X-ray–based kinematic measures.

After biplane X-ray testing, a CT image of the subject's cervical spine from C3 to the first thoracic vertebrae (T1) was acquired. Imaging parameters included a field of view of 130 mm, a 512×512 reconstruction matrix, and a voxel size of $0.25\times0.25\times1.25$ mm. Individual 3D bone models of C4, C5, C6, and C7 were created by manually segmenting each vertebra from other surrounding bones and soft tissues.

The 3D position and orientation of each vertebra were determined from the biplane X-ray images using the model-based tracking technique [20]. An anatomical coordinate system was created for each vertebra using anatomical landmarks and vector cross products as previously described (Fig. 2). The 3D translations and rotations of each pair of vertebrae (ie, C4–C5, C5–C6, and C6–C7) were calculated using the positions and orientations determined with model-based tracking. Specifically, the six kinematic outcome measures included lateral bending, flexion-extension, axial rotation, AP translation, LR translation, and SI translation.

Intervertebral rotations (determined from the biplane X-ray images) were plotted against neck extension angle (determined from the video-based motion capture system) for the neck extension motion task. Similarly, intervertebral rotations were plotted against axial neck rotation angle for the axial neck rotation motion task. For each motion task, total rotational range of motion about each anatomical axis was calculated and averaged across the three trials. A *t* test compared the total range of motion about each axis to zero, with significance set at $p<.05$.

Results

Validation of model-based tracking technique

The model-based tracking technique produced results that were in excellent agreement with the RSA technique. For translational accuracy, bias ranged from 0.10 to 0.56 mm and was not significantly different than zero (Table 1, $p=.30$). Precision was less than ±0.15 mm, and dynamic accuracy was within ±0.56 mm (Table 1). For rotational accuracy, bias ranged from -0.89° to 0.63° and was not significantly different than zero (Table 2, $p=.49$). Precision was less than $\pm0.26^\circ$ and dynamic accuracy was less than $\pm0.61^\circ$ for the predominant rotations associated with the flexion-extension and axial rotation tasks (Table 2). Thus, this study demonstrated that the model-based tracking technique is capable of measuring cervical spine motion

Table 1
Translational accuracy characterized in terms of bias, precision, and overall dynamic accuracy

	Applied motion	
Translation	Flexion-extension	Axial rotation
Bias		
AP translation	0.56±0.33	0.10±0.21
LR translation	0.34±0.21	0.23±0.11
SI translation	0.32±0.12	0.44±0.17
Precision		
AP translation	0.12	
LR translation	0.11	
SI translation	0.15	
Dynamic accuracy		
AP translation	0.56±0.32	0.23±0.17
LR translation	0.35±0.18	0.23±0.11
SI translation	0.32±0.12	0.44±0.17

AP, anterior-posterior; LR, left-right; SI, superior-inferior.
All data are expressed in millimeters.

to within ±0.56 mm and ±0.61°. These findings are consistent with previous validation studies conducted in our laboratory that have reported the accuracy of the model-based tracking technique to be within ±0.4 to ±0.6 mm and ±0.5° to ±0.9° for the glenohumeral [20], tibiofemoral [23], and patellofemoral joints [24].

In vivo application

For the neck extension motion task (Fig. 1, left), the predominant rotation for all three motion segments was in flexion-extension with a near-linear relationship between neck extension angle and intervertebral flexion-extension angle (R^2=0.99, Fig. 3). However, lateral bending and axial rotation also occurred during this motion task (Fig. 3). The total rotational range of motion for each of the three motion segments was significantly greater than zero for flexion-extension, lateral bending, and axial rotation ($p<.001$, Fig. 4). Flexion-extension range of motion ranged from

Table 2
Rotational accuracy characterized in terms of bias, precision, and overall dynamic accuracy

	Applied motion	
Rotation	Flexion-extension	Axial rotation
Bias		
Lateral bending	−0.01±0.18	0.32±0.24
Flexion-extension	−0.49±0.57	−0.89±0.55
Axial rotation	0.63±0.72	0.51±0.44
Precision		
Lateral bending	0.10	
Flexion-extension	0.24	
Axial rotation	0.26	
Dynamic accuracy		
Lateral bending	0.14±0.12	0.35±0.20
Flexion-extension	0.61±0.44	0.90±0.54
Axial rotation	0.85±0.43	0.55±0.40

All data are expressed in degrees.

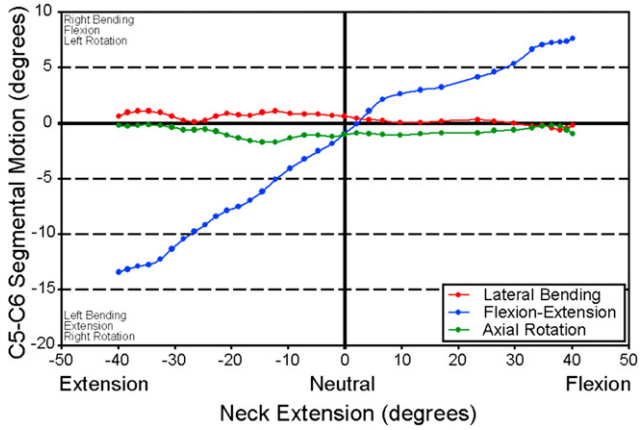

Fig. 3. Rotations of C5 relative to C6 are plotted versus neck extension angle during a single neck extension motion task. There was a near-linear relationship between neck extension angle and C5–C6 flexion-extension angle (R^2=0.99). For lateral bending (rotation about the anterior-posterior axis), positive values indicate right lateral bending and negative values indicate left lateral bending. For flexion-extension (rotation about the ML-axis), positive values indicate flexion and negative values indicate extension. For axial rotation (rotation about the SI-axis), positive values indicate left rotation and negative values indicate right rotation.

a minimum of 17.4±0.9° at the C6–C7 motion segment to a maximum of 28.9±0.7° at C5–C6 (Fig. 4). Lateral bending range of motion was much more consistent across motion segments, ranging from a minimum of 3.2±0.6° at C6–C7 to a maximum of 4.2±0.7° at C4–C5 (Fig. 4). Similarly, the range of motion for axial rotation varied from a minimum of 2.5±0.6° at C6–C7 to a maximum of 3.3±0.3° at C4–C5 (Fig. 4).

For the neck extension motion task (Fig. 1, left), the translational range of motion was significantly greater than zero for each motion segment along each of the anatomical directions ($p<.01$, Fig. 5). For the C4–C5 motion segment,

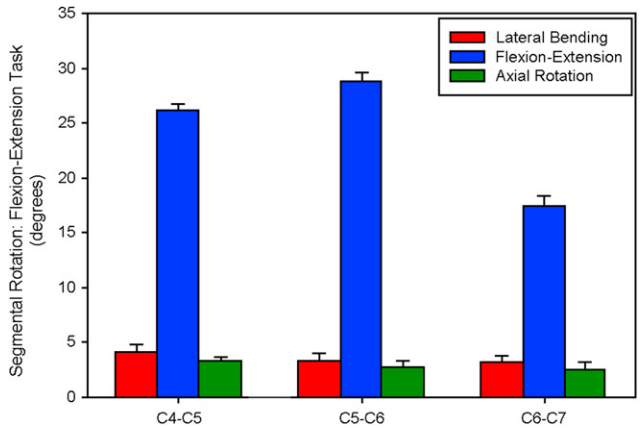

Fig. 4. Maximum rotational range of motion for the three vertebral motion segments (C4–C5, C5–C6, and C6–C7) during the neck extension motion task. For each motion segment, the mean and standard deviation across three trials are shown. Flexion-extension was the predominant rotation, but all rotational ranges of motion (ie, flexion-extension, lateral bending, and axial rotation) were significantly greater than zero ($p<.01$). All data are reported in degrees.

AP translation (6.0±0.4 mm) was considerably greater than either LR translation (1.9±0.6 mm) or SI translation (1.6±0.2 mm, Fig. 5). This finding was consistent for C5–C6, with AP translation (6.1±0.1 mm) appreciably higher than either LR translation (1.5±0.2 mm) or SI translation (1.6±0.3 mm, Fig. 5). However, the translations at the C6–C7 were much more consistent, varying from a minimum of 1.6±0.6 mm in LR translation to a maximum of 2.9±0.2 mm in AP translation (Fig. 5).

For the axial neck rotation motion task (Fig. 1, right), there was a complex pattern of segmental rotations that involved lateral bending, flexion-extension, and axial rotation (Fig. 6). Each of the three motion segments had rotations whose total ranges of motion were significantly greater than zero ($p<.02$, Fig. 7). For the C4–C5 motion segment, the predominant rotation was in lateral bending with a total range of motion of 10.7±2.3°, with smaller amounts of flexion-extension (4.2±0.9°) and axial rotation (5.2±1.0°, Fig. 7). The C5–C6 motion segment demonstrated similar results, with total range of motion occurring primarily in lateral bending (9.2±3.0°) and less motion in flexion-extension (3.4±1.5°) and axial rotation (3.8±0.6°, Fig. 7). Rotations at C6–C7 were more consistent across the three anatomical axes, with total range of motion varying from a minimum of 2.2±0.4° in axial rotation to a maximum of 4.0±1.5° in lateral bending (Fig. 7).

For the axial neck rotation motion task (Fig. 1, right), the translational range of motion was also significantly greater than zero for each of the three motion segments ($p<.03$, Fig. 8). Translations were small during this motion task, with total translational range of motion ranging from a minimum of 0.4±0.1 mm of SI translation for C5–C6 to a maximum of 1.3±0.5 mm of LR translation for C4–C5 (Fig. 8).

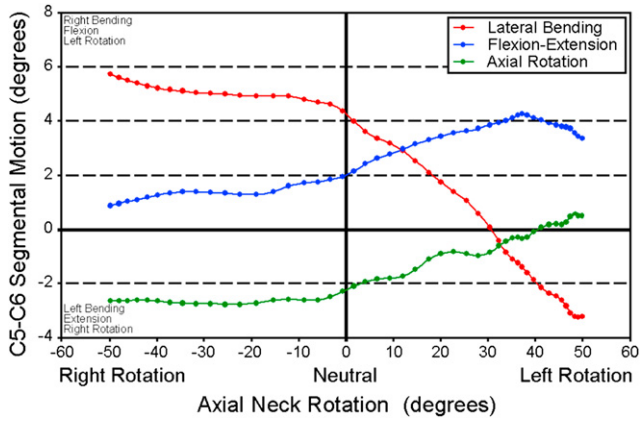

Fig. 6. Rotations of C5 relative to C6 are plotted versus neck axial rotation angle for a single axial neck rotation motion task. Coupled rotations are evident about all three anatomical axes, with lateral bending being the predominant rotation. For lateral bending (rotation about the anterior-posterior axis), positive values indicate right lateral bending and negative values indicate left lateral bending. For flexion-extension (rotation about the ML-axis), positive values indicate flexion and negative values indicate extension. For axial rotation (rotation about the SI-axis), positive values indicate left rotation and negative values indicate right rotation.

Discussion

The objectives of this study were to characterize the translational and rotational accuracy of a model-based tracking technique for measuring cervical spine motion and to demonstrate its in vivo application. Using a well-validated and well-accepted dynamic RSA technique [17] as a gold standard, this study demonstrated that the model-based tracking technique is capable of measuring cervical spine motion to within ±0.6 mm in translation and ±0.6° in rotation. In addition, the study demonstrated in vivo application of the measurement technique and

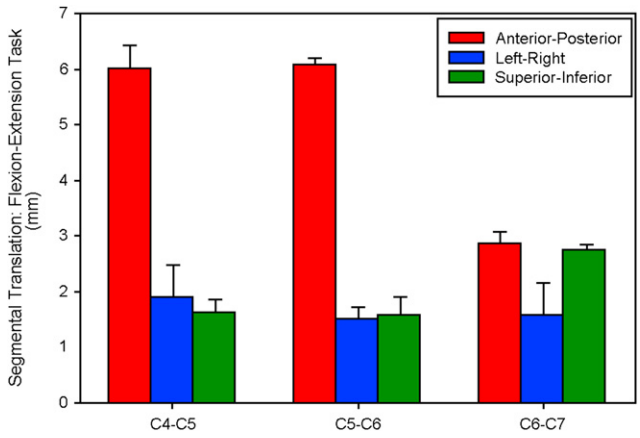

Fig. 5. Maximum translational range of motion for the three vertebral motion segments (C4–C5, C5–C6, and C6–C7) during the neck extension motion task. For each motion segment, the mean and standard deviation across three trials are shown. Anterior-posterior translation was the predominant translation for C4–C5 and C5–C6. All translational ranges of motion (ie, anterior-posterior, left-right, and superior-inferior) were significantly greater than zero for each motion segment ($p<.01$). All data are reported in millimeters.

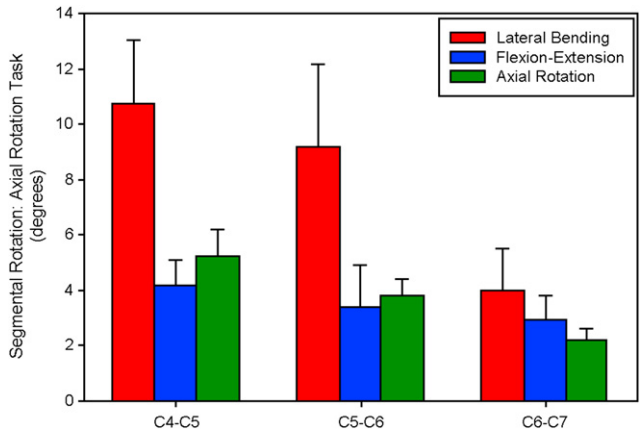

Fig. 7. Maximum rotational range of motion for the three vertebral motion segments (C4–C5, C5–C6, and C6–C7) during the axial neck rotation motion task. For each motion segment, the mean and standard deviation across three trials are shown. Lateral bending was the predominant rotation for all three motion segments, but all rotational ranges of motion (ie, flexion-extension, lateral bending, and axial rotation) were significantly greater than zero ($p<.05$). All data are reported in degrees.

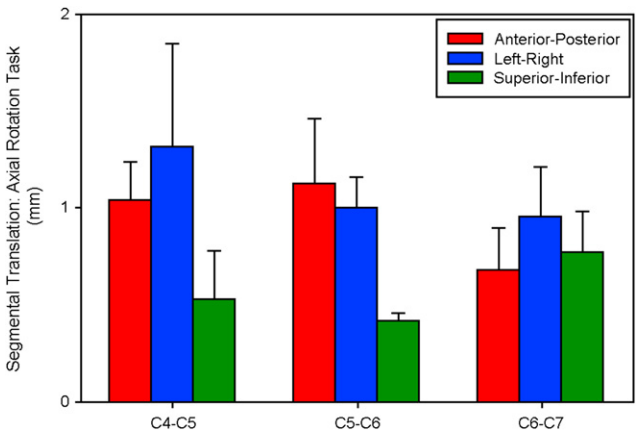

Fig. 8. Maximum translational range of motion for the three vertebral motion segments (C4–C5, C5–C6, and C6–C7) during the axial neck rotation motion task. For each motion segment, the mean and standard deviation across three trials are shown. Translations were statistically greater than zero along each axis for all motion segments ($p<.05$), although there was no prominent trend in any direction. All data are reported in millimeters.

reported the results from one subject that was in substantial agreement with previous literature [6–8,25–31].

The in vivo results acquired during the neck extension motion task in this study were in agreement with the previously reported data. For example, flexion-extension in the lower cervical spine has been previously reported to range from 16° to 23° at C4–C5, 15° to 28° at C5–C6, and 11° to 21° at C6–C7 [7,8,25–28,30]. In comparison, the data from the present study reported ranges of motion of 26.2°±0.6° at C4–C5, 28.9°±0.7° at C5–C6, and 17.4°±0.9° at C6–C7 (Fig. 4). For the axial neck rotation motion task, previous research has reported axial rotation of the cervical spine to range from 4° to 7° at C4–C5, 5° to 7° at C5–C6, and 2° to 6° at C6–C7 [6,29,31]. In comparison, the data from this study reported ranges of motion of 5.2°±1.0° for C4–C5, 3.8°±0.6° for C5–C6, and 4.0°±1.5° for C6–C7 (Fig. 7).

Much of our understanding of in vivo cervical spine motion has been based on studies conducted using conventional radiographs [5–9,30,31]. These studies have typically acquired radiographs with the neck positioned in one of several static positions (eg, full flexion and full extension) and then manually calculated angles between the adjacent vertebrae at each neck position. This approach assumes that the maximum range of motion between the cervical vertebrae will occur at the end ranges of neck motion. However, the preliminary data presented here suggest that this may not always be true. Specifically, the data for this subject indicate that maximum flexion of C5–C6 during the axial neck rotation motion task does not occur at the neck position of maximum left rotation but rather at approximately 10°–15° less than the neck position of maximum left rotation (Fig. 6). Consequently, conventional approaches that analyze cervical spine motion at end ranges of neck motion may actually underestimate the true range of cervical spine motion. Therefore, measuring cervical spine motion using biplane X-ray images that were acquired at a high sampling rate (60 images/second) is a particular strength of this approach and allows us to more carefully discern complex motion patterns that may be masked by static imaging techniques.

Another limitation of conventional radiographic studies of cervical spine motion is that they typically provide only 2D measures of joint motion. Consequently, these studies have been limited to studying motions that are believed to be largely planar. For example, a large number of studies have only investigated range of motion during neck flexion-extension [5–9]. Although the rationale for investigating this motion may be that flexion-extension of the cervical spine is clinically relevant, it is also likely that flexion-extension is investigated with such high frequency because it is a motion that potentially minimizes the out-of-plane errors that are inherent to 2D measurement techniques [32,33]. Consequently, these 2D imaging techniques are unable to accurately measure complex motion patterns, such as the axial neck rotation motion task, that involve significant rotations around each of the anatomical axes (Fig. 6 and Fig. 7). In contrast, the biplane X-ray approach described here is capable of accurately measuring 3D joint motion and is therefore well suited for studying a wide range of clinically relevant neck motions.

More advanced techniques have been reported for measuring 3D motion of the spine under in vivo conditions. However, the level of rigor with which the accuracy of the measurement technique is determined seems to vary significantly. For example, Mimura et al. [29] reported a technique for measuring 3D motion of the cervical spine during axial rotation of the neck. Their technique, which involved acquiring static biplane radiographic images at fixed neck positions and then manually digitizing specific anatomical landmarks, was reported to be accurate to within 1.0 mm for translations and 1.5° for rotations [29]. However, the manner in which the accuracy of this technique was determined was not reported in a full-length publication, and consequently, it is impossible to determine if the condition of their accuracy assessment was a realistic simulation of in vivo conditions. Wang et al. [18] described a dual fluoroscopy technique for measuring spine kinematics. Although the authors provided a thorough analysis of translational accuracy (±0.4 mm) by comparing measured translations and velocities to those imposed by a material testing machine, rotational accuracy of this technique was not reported and is therefore unknown. For the present study, we assessed both the translational and rotational accuracy of the technique by comparing the model-based tracking technique with dynamic RSA and reporting the errors in terms of bias, precision, and overall dynamic accuracy. Anderst et al. [17] used dynamic RSA to measure motion of the lumbar spine [17]. This approach, which involves tracking the 3D position of surgically implanted tantalum beads from biplane X-ray images, is reported to be

accurate to within ±0.18 mm in translation and ±0.26° in rotation. Using dynamic RSA as the gold standard comparison, the model-based tracking technique was determined to be accurate to within ±0.6 mm and ±0.6° for measuring cervical spine motion.

The strength of the experimental approach described here is that it provides accurate noninvasive measures of in vivo cervical spine motion during dynamic activities. The limitation of this approach is that radiation safety concerns restrict the number of trials that can be acquired for a given subject. In addition, the size of the biplane X-ray system's 3D field of view, which is defined by the region of overlap between the crossing X-ray beams, limits the activities during which cervical spine motion can be measured.

This study examined the accuracy of a model-based tracking technique for measuring cervical spine motion during neck extension and axial neck rotation motion activities. The in vitro validation indicated that this method is accurate to within ±0.6 mm in translation and ±0.6° in rotation. Using this technique, we presented preliminary data on in vivo cervical spine motion that are in agreement with previous studies. It is anticipated that this experimental approach will enhance our understanding of cervical spine kinematics in normal asymptomatic subjects and will help to characterize the effects of surgical procedures such as spinal fusion or artificial disc replacement.

Acknowledgments

The authors acknowledge the funding provided by the Department of Orthopaedic Surgery at Henry Ford Hospital.

References

[1] Syed FI, Oza AL, Vanderby R, et al. A method to measure cervical spine motion over extended periods of time. Spine 2007;32:2092–8.
[2] Walmsley RP, Kimber P, Culham E. The effect of initial head position on active cervical axial rotation range of motion in two age populations. Spine 1996;21:2435–42.
[3] Fuller DA, Kirkpatrick JS, Emery SE, et al. A kinematic study of the cervical spine before and after segmental arthrodesis. Spine 1998;23: 1649–56.
[4] Panjabi MM, Miura T, Cripton PA, et al. Development of a system for in vitro neck muscle force replication in whole cervical spine experiments. Spine 2001;26:2214–9.
[5] Baba H, Furusawa N, Imura S, et al. Late radiographic findings after anterior cervical fusion for spondylotic myeloradiculopathy. Spine 1993;18:2167–73.
[6] Dvorak J, Hayek J, Zehnder R. CT-functional diagnostics of the rotatory instability of the upper cervical spine. Part 2. An evaluation on healthy adults and patients with suspected instability. Spine (Phila Pa 1976) 1987;12:726–31.
[7] Dvorak J, Froehlich D, Penning L, et al. Functional radiographic diagnosis of the cervical spine: flexion/extension. Spine 1988;13:748–55.
[8] Dvorak J, Panjabi MM, Novotny JE, et al. In vivo flexion/extension of the normal cervical spine. J Orthop Res 1991;9:828–34.
[9] Elsawaf A, Mastronardi L, Roperto R, et al. Effect of cervical dynamics on adjacent segment degeneration after anterior cervical fusion with cages. Neurosurg Rev 2009;32:215–24.
[10] Ishii T, Mukai Y, Hosono N, et al. Kinematics of the upper cervical spine in rotation: in vivo three-dimensional analysis. Spine 2004;29: E139–44.
[11] Ishii T, Mukai Y, Hosono N, et al. Kinematics of the cervical spine in lateral bending: in vivo three-dimensional analysis. Spine 2006;31:155–60.
[12] Lin RM, Tsai KH, Chu LP, et al. Characteristics of sagittal vertebral alignment in flexion determined by dynamic radiographs of the cervical spine. Spine 2001;26:256–61.
[13] Miyazaki M, Hong SW, Yoon SH, et al. Kinematic analysis of the relationship between the grade of disc degeneration and motion unit of the cervical spine. Spine 2008;33:187–93.
[14] Simon S, Davis M, Odhner D, et al. CT imaging techniques for describing motions of the cervicothoracic junction and cervical spine during flexion, extension, and cervical traction. Spine 2006;31:44–50.
[15] Liu F, Cheng J, Komistek RD, et al. In vivo evaluation of dynamic characteristics of the normal, fused, and disc replacement cervical spines. Spine 2007;32:2578–84.
[16] Morishita Y, Hida S, Miyazaki M, et al. The effects of the degenerative changes in the functional spinal unit on the kinematics of the cervical spine. Spine 2008;33:E178–82.
[17] Anderst WJ, Vaidya R, Tashman S. A technique to measure three-dimensional in vivo rotation of fused and adjacent lumbar vertebrae. Spine J 2008;8:991–7.
[18] Wang S, Passias P, Li G, et al. Measurement of vertebral kinematics using noninvasive image matching method—validation and application. Spine 2008;33:E355–61.
[19] Tashman S, Anderst W. In-vivo measurement of dynamic joint motion using high speed biplane radiography and CT: application to canine ACL deficiency. J Biomech Eng 2003;125:238–45.
[20] Bey MJ, Zauel R, Brock SK, et al. Validation of a new model-based tracking technique for measuring three-dimensional, in vivo glenohumeral joint kinematics. J Biomech Eng 2006;128:604–9.
[21] Stokes IA. Three-dimensional terminology of spinal deformity. A report presented to the Scoliosis Research Society by the Scoliosis Research Society Working Group on 3-D terminology of spinal deformity. Spine 1994;19:236–48.
[22] ASTM. Standard practice for use of the terms precision and bias in ASTM test methods. West Conshohocken: American Society for Testing and Materials, 1996.
[23] Anderst W, Zauel R, Bishop J, et al. Validation of three-dimensional model-based tibio-femoral tracking during running. Med Eng Phys 2009;31:10–16.
[24] Bey MJ, Kline SK, Tashman S, et al. Accuracy of biplane x-ray imaging combined with model-based tracking for measuring in-vivo patellofemoral joint motion. J Orthop Surg Res 2008;3:38.
[25] Aho A, Vartiainen O, Salo O. Segmentary antero-posterior mobility of the cervical spine. Ann Med Intern Fenn 1955;44:287–99.
[26] Bhalla SK, Simmons EH. Normal ranges of intervertebral-joint motion of the cervical spine. Can J Surg 1969;12:181–7.
[27] Holmes A, Wang C, Han ZH, et al. The range and nature of flexion-extension motion in the cervical spine. Spine 1994;19:2505–10.
[28] Lind B, Sihlbom H, Nordwall A, et al. Normal range of motion of the cervical spine. Arch Phys Med Rehabil 1989;70:692–5.
[29] Mimura M, Moriya H, Watanabe T, et al. Three-dimensional motion analysis of the cervical spine with special reference to the axial rotation. Spine 1989;14:1135–9.
[30] Penning L. Normal movements of the cervical spine. AJR Am J Roentgenol 1978;130:317–26.
[31] Penning L, Wilmink JT. Rotation of the cervical spine. A CT study in normal subjects. Spine 1987;12:732–8.
[32] Banks SA, Hodge WA. Accurate measurement of three-dimensional knee replacement kinematics using single-plane fluoroscopy. IEEE Trans Biomed Eng 1996;43:638–49.
[33] Moro-oka TA, Hamai S, Miura H, et al. Can magnetic resonance imaging-derived bone models be used for accurate motion measurement with single-plane three-dimensional shape registration? J Orthop Res 2007;25:867–72.